Available online at www.sciencedirect.com
ScienceDirect
Journal of Power Sources 177 (2008) 61–66
JOURNAL OF POWER SOURCES
www.elsevier.com/locate/jpowsour

Short communication

Improved performance of Pd electrocatalyst supported on ultrahigh surface area hollow carbon spheres for direct alcohol fuel cells

Feng Ping Hu [a], Zhenyou Wang [a], Yongliang Li [a], Changming Li [b], Xin Zhang [c], Pei Kang Shen [a,*]

[a] *State Key Laboratory of Optoelectronic Materials and Technologies, School of Physics and Engineering, Sun Yat-Sen University, Guangzhou 510275, PR China*
[b] *School of Chemical and Biomedical Engineering, Nanyang Technological University, Singapore 637457, Singapore*
[c] *Department of Chemistry, Shantou University, Shantou 515063, PR China*

Received 4 October 2007; received in revised form 7 November 2007; accepted 7 November 2007
Available online 17 November 2007

Abstract

Ultrahigh surface area hollow carbon spheres (HCSs) with open micropores and nanochannels have been prepared by combined methods of hydrothermal and intermittent microwave heating (IMH) for the first time. It is found that the addition of poly(ethylene glycol)-block-poly(propylene glycol)-block-poly(ethylene glycol) (P123) leads to a large BET surface area of 1249.3 $m^2 g^{-1}$. The catalytic activity of Pd supported on HCS is over 3 times higher than that on Pd supported on commercial Vulcan XC-72 carbon at the same Pd loadings. It is proven that the higher catalytic activity is contributed from the formation of the high electrochemical active surface area (EASA) which is due to the hollow carbon structure with open micropores and nanochannels.

Keywords: Hollow carbon spheres; Liquid fuel cells; Template; Ethanol oxidation; Polystyrene spheres

1. Introduction

The different structured or shaped carbon materials such as onion-like carbon [1], flower-like carbon [2], straw-like carbon [3] and nanorods carbon [4] have been of continuous research interest since carbon nanotubes were found in 1991 [5]. This new class carbon materials have been used for conductive and high-strength composites [6], gas/energy storage [7], catalyst support [8] and adsorbents [9] because of their intrinsic properties involving large BET surface area, low weight, self-sinter, chemical inertia and excellent electronic conductivity and so on. As we know, the catalyst supports should meet the requirements of high conductivity and large surface area to improve the dispersion of the catalyst and catalytic activity. Our previous studies revealed that the material with hollow structure and large mesopores as electrocatalyst support could effectively improve the performance of electrocatalyst [10–13]. Several carbon materials such as spherical carbon capsules [5], hollow carbon nanospheres [14], active fiber carbon (AFC) [15], mesostructured carbon materials [16] were used as supports of Pt or Pd electrocatalysts due to their large surface area and high stability. It is well known that the activity of the electrocatalyst could be enhanced by increasing the electrochemical three-phase interface. Carbon materials with high BET surface area does not mean a high electrochemical active surface area (EASA) since the liquid sealing effect in electrochemical situation or in liquid fuel cells. Our original idea is to obtain the high surface area hollow carbon spheres by opening the micropores or nanochannels on carbon. In that case, the metal catalysts could be deposited in the pores and channels and at the same time the liquid could transport through those open ways to tremendously increase the three-phase interface. This novel idea strategically opens a new way to make electrocatalysts with ultrahigh electrochemical active surface area.

In view of the electrocatalyst used in fuel cells, the higher surface areas and larger pore volumes of the support materials allow

* Corresponding author. Tel.: +86 20 84036736; fax: +86 20 84113369.
E-mail address: stsspk@mail.sysu.edu.cn (P.K. Shen).

0378-7753/$ – see front matter © 2007 Elsevier B.V. All rights reserved.
doi:10.1016/j.jpowsour.2007.11.024

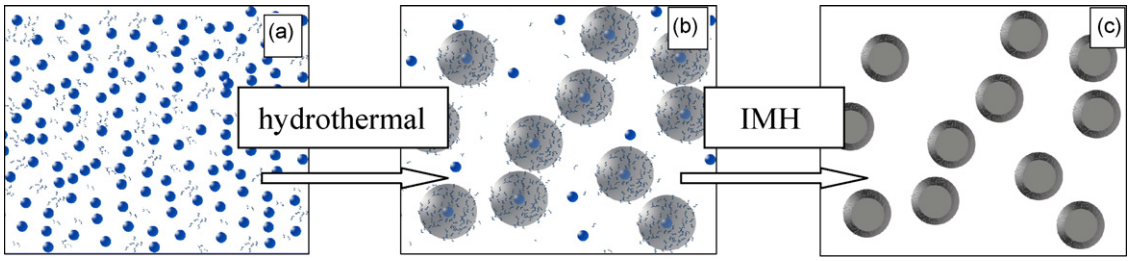

Fig. 1. Schematic illustration of the synthesis procedure of HCSs.

a better dispersion for the precious metal catalysts and provide an open network around the active catalysts for facile diffusion of fuels and products [8]. On the other hand, in order to accelerate the commercialization of the fuel cells, special attention has been focused on the development of Pt-free electrocatalysts with high efficiency to alleviate the dependence on the precious metals and to reduce the cost [17,18]. Pd-based electrocatalysts showed extremely high activity for the oxidation of alcohols in alkaline solutions [12,15,19,20], particularly, for the oxidation of ethanol. The significance is that Pd is much cheaper and is at least 50 times more available in the earth than Pt [21].

There are numerous routes to prepare hollow carbon spheres (HCSs) such as template [22], pyrolysis [23], reduction [24] and hydrothermal [25] methods. However, these methods are either time-consuming or rather complicated. Here, we report an easy method to prepare HCSs with polystyrene spheres (PSs) as template along with the decomposition of glucose in P123 surfactant containing solution under hydrothermal conditions. An intermittent microwave heating (IMH) technique was first adopted to rapidly form the hollow carbon spheres [26]. With the removal of the trapped P123 molecules during the IMH treatment, large amount of open pores and nanochannels formed. The novelty of this work is that the HCSs prepared by the present method give extremely high BET surface area. More importantly, Pd electrocatalyst supported on such ultrahigh surface area HCSs gives significantly high electrochemical active surface area and tremendously high activity for alcohol oxidation.

2. Experimental

Polystyrene spheres (PSs) were widely used as the template to synthesize hollow metal oxide or metal nanomaterials [27,28]. In this study, PS was obtained by emulsifier-free dispersion polymerization of styrene and used to synthesize hollow carbon spheres. Typically, 40 ml of 1 mol dm^{-3} glucose and 5 ml of 20 wt% PS in poly(ethylene glycol)-block-poly(propylene glycol)-block-poly(ethylene glycol) (P123, Aldrich, USA) containing solution (2 ml, 50 mg ml^{-1} P123) were added into 50 ml autoclave and heated at 180 °C for 12 h. The deposit was then washed with ethanol and distilled water and dried at 80 °C for 2 h. Subsequently, the product was heated in microwave oven at a procedure of 2 min on and 1 min off and 2 min on again. The synthesis procedure is schematically illustrated in Fig. 1.

The first step is to mix glucose and PS in the presence of P123 prior to the hydrothermal reaction. The PS/C core–shell structure formed during the hydrothermal reaction. At the same time, the P123 molecules were trapped in the carbon layers during the formation of carbon shell. Finally, the P123 molecules were removed along with the removal of PS by IMH treatment in air, leaving large amount of open micropores and nanochannels.

Pd supported on HCS (denoted as Pd/HCS) was prepared and used as electrocatalyst for oxidation of alcohols. Pd/HCS and Pd/C electrocatalysts were prepared by reducing $PdCl_2$ aqueous solution (4.7 ml, 0.1 mol dm^{-3}) on 50.0 mg carbon or HCS. The formic acid (5 ml, 1 mol dm^{-3}) was used as reducing reagent. The mixture was put into a microwave oven (1000 W, 2.45 GHz, Galanz, China) and was then alternatively heated for 20 s and paused for 60 s for 6 times. The Pd loadings on the Pd/C and Pd/HCS electrodes were both controlled at 0.3 mg cm^{-2} [11].

Chemicals were of analytical grade and used as received. The experiments were carried out at 30 °C controlled by a water-bath thermostat. Structural characterization was conducted on a JOEP JEM-2010 (JEOL Ltd.) transmission electron microscopy (TEM) operating at 200 kV, and an X-ray diffractometer (D/Max-IIIA, Rigaku Co., Japan, Cu K_1 ($\lambda = 1.54056$ Å) radiation). All electrochemical measurements were performed in a three-electrode cell on an IM6e electrochemical workstation (Zahner-Electrik, Germany). A platinum foil (3.0 cm^2) and Hg/HgO (1.0 mol dm^{-3} KOH) were used as counter and reference electrodes, respectively.

3. Results and discussion

Fig. 2 shows the TEM images of HCS and Pd/HCS. The hollow nature of the carbon spheres with uniform size distribution of ~1.5 μm is clearly shown in Fig. 2a. The wall thickness of the hollow spheres is around 150 nm as shown in Fig. 2b. In fact, the diameter of the as-prepared PS/C core–shell structure is around 3 μm (see Fig. 2c). Therefore, it is clear that the thickness of the carbon wall was reduced from both interior and exterior surfaces along with the decomposition of PS core during the microwave irradiation in air. This reveals that the micropores or nanochan-

Table 1
Structural characteristics of HCS

Sample	HCS (with P123)	HCS (without P123)
BET (m^2 g^{-1})	1249.3	732.1
Micropore area (m^2 g^{-1})	886.2	612.2
Total pore volume (cm^3 g^{-1})	0.638	0.499
Micropore volume (cm^3 g^{-1})	0.412	0.284
Average pore diameter (nm)	0.573	0.483

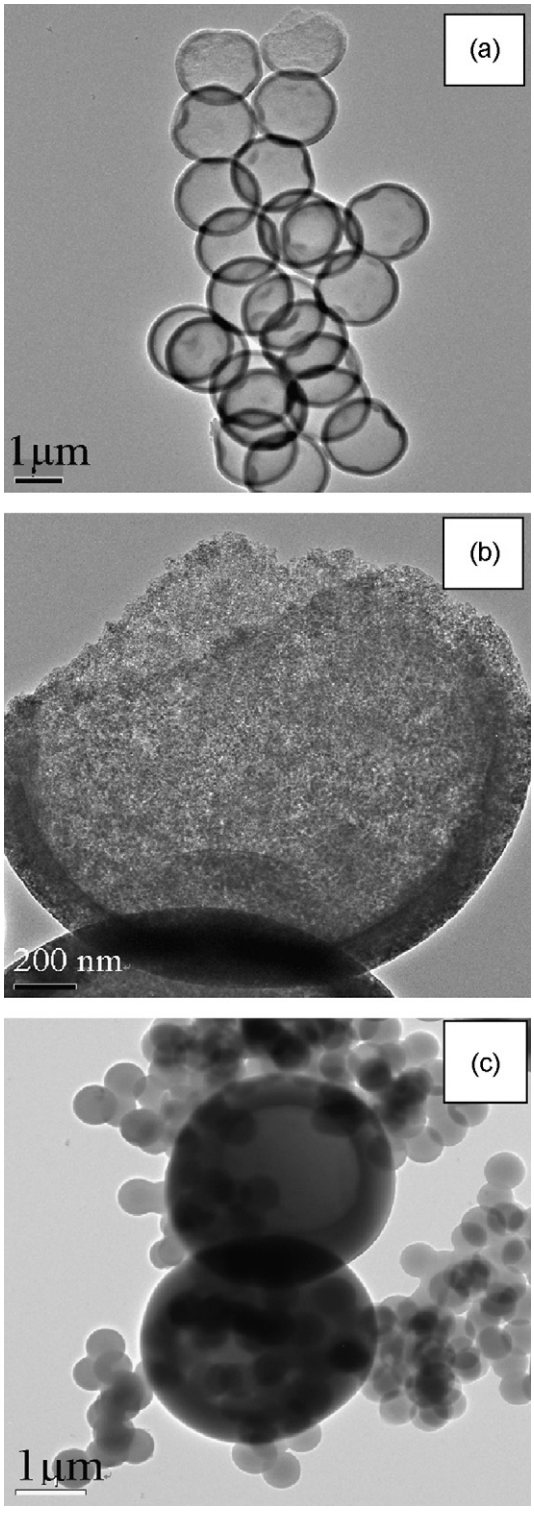

Fig. 2. TEM images of (a) HCS (bar 1 μm), (b) the broken HCS with enlarged scale (bar 200 nm) and (c) carbon spheres before the IMH treatment (bar 1 μm).

nels on the hollow carbon spheres are opened during the removal of PS, which allows the air (oxygen) diffuse into the inside to react with carbon on the interior wall.

The surface areas and structural characteristics of the hollow carbon spheres prepared with and without P123 were measured and summarized in Table 1. It shows an ultrahigh surface area

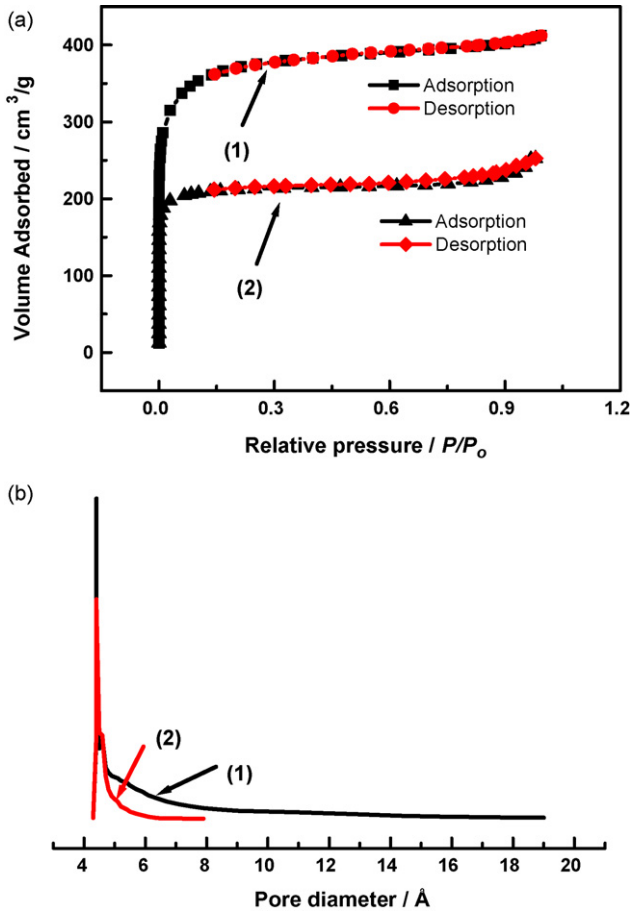

Fig. 3. (a) N_2 adsorption isotherms of HCS prepared with (1) and without (2) P123 and (b) pore size distribution of HCS prepared with (1) and without (2) the addition of P123.

of 1249.3 $m^2\ g^{-1}$ for the HCS prepared in the presence of P123 against 732.1 $m^2\ g^{-1}$ for the HCS prepared without the addition of P123. Fig. 3a shows the N_2 adsorption isotherms of the HCS prepared with and without P123. They show the same type I isotherm. The overlap of the adsorption and desorption curves indicate the presence of micropores. However, the transition from the rapid raise to the flat platform of the curve is relatively slow for the HCS prepared with P123, indicating the existence of larger micropores. The pore distribution and the pore size were measured and the results are shown in Fig. 3b. The pore size is ranging from 0.4 to 0.6 nm in diameter for the HCSs prepared without P123. However, the distribution of the pores was broadened and the size increased to 0.8 nm in diameter for the HCSs prepared with P123. XRD measurement showed that both XC-72R carbon (Cabot Corp., USA) and HCS prepared in this study are amorphous structured with small crystallization.

The average pore diameters of the HCSs prepared with and without the addition of P123 are 0.573 and 0.483 nm as summarized in Table 1. The pore volumes of the HCSs prepared with and without the addition of P123 are 0.412 and 0.284 $cm^3\ g^{-1}$, respectively. It is clear that the addition of P123 tremendously increased the pore number and the pore size which is the main contributor to the ultrahigh surface area. We failed to further

increase the surface area of the prepared HCS by adding more P123. Thick foam formed during the stirring of the glucose/PS mixture with higher P123 concentrations and the mixture was gradually stuck together.

The HCSs were used as support to prepare Pd-based electrocatalysts for alcohol oxidation. The Pd distribution on a single HCS particle was observed by TEM as shown in Fig. 4a. The agglomeration of Pd particles is observed on the surface of HCS (Fig. 4b). The agglomerated particle size is around 20 nm as shown in Fig. 4c.

The catalytic activity of Pd/HCS for the oxidation of ethanol was tested. Fig. 5a shows the cyclic voltammograms of ethanol oxidation on Pd/C and Pd/HCS electrodes. The smooth Pd electrode was used to compare the electrochemical active surface area. Pd is active for ethanol oxidation in alkaline solution as previously reported [19]. The characteristic peaks for ethanol oxidation appear on the CV curve as shown in the inset of Fig. 5a though the current densities are small. The Pd/HCS shows extremely higher activity for ethanol oxidation compared to that of Pd/C in terms of the onset potential and peak current density. The peak current density of ethanol oxidation on Pd/HCS electrocatalyst is 3.7 times higher than that on Pd/C electrocatalyst. The mechanistic investigation on the nature of the high activity of ethanol oxidation on Pd/HCS is in progress. The effect of the surface area on the catalytic activity should be considered. To the electrolysis, the electrochemical active surface area is more important than the BET surface area. Fig. 5b compares the EASAs of different electrodes in the background solution. The electrochemical active surface areas of metal Pd, Pd/C and Pd/HCS are 0.287, 1.913 and 10.718 mC cm^{-2}, respectively. The EASA ratios between Pd/HCS to Pd/C and Pd are 5.6 and 37. However, the ratios of the peak current densities for ethanol oxidation between Pd/HCS to Pd/C and Pd are 3.7 and 35, respectively. The smaller ratio of the peak current densities for ethanol oxidation between Pd/HCS to Pd/C is mainly due to the more serious concentration polarization on Pd/HCS at high current densities.

The electrode structured by the micrometer sized HCS support is beneficial for the mass transport of the ethanol from the bulk to the inner layers of the electrocatalyst. We performed an experiment by integrating the anodic peak charges for ethanol oxidation during the forward potential cycling at different scan rates. The relationship between peak charge and scan rate on Pd/C electrode and Pd/HCS electrode are shown in Fig. 5c. Q_v represents the integrated charge of the anodic peak for ethanol oxidation at different scan rates. Q_{max} denotes the charge obtained at the scan rate of 2 mV s^{-1}. The ratios of Q_v/Q_{max} of both the electrodes decrease with the increase in the scan rate. However, the decrease on Pd/HCS electrode is much slow at the scan rate lower than 100 mV s^{-1}, indicating that the mass transport on Pd/HCS electrode is faster than that on Pd/C electrode. The results indicate that the oxidation of ethanol on Pd/HCS electrode is controlled by activation polarization at lower scan rates because the microporous structure makes ethanol to access the active sites easier. This is further proven by plotting the peak current density against the square root of the scan rate as shown in the inset of Fig. 5c. It shows a straight line on Pd/C electrode

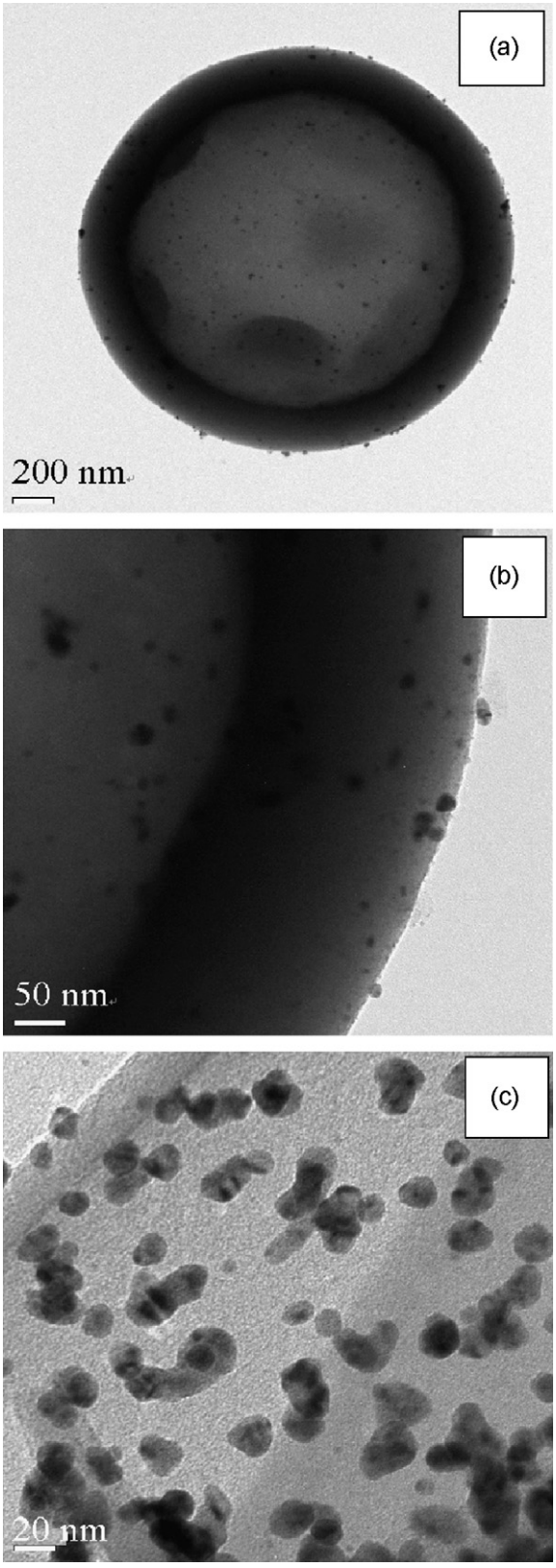

Fig. 4. (a) TEM image of Pd/HCS electrocatalyst (bar 200 nm), (b) the distribution of Pd on the surface of HCS (bar 50 nm) and (c) the enlarged TEM image of Pd/HCS (bar 20 nm).

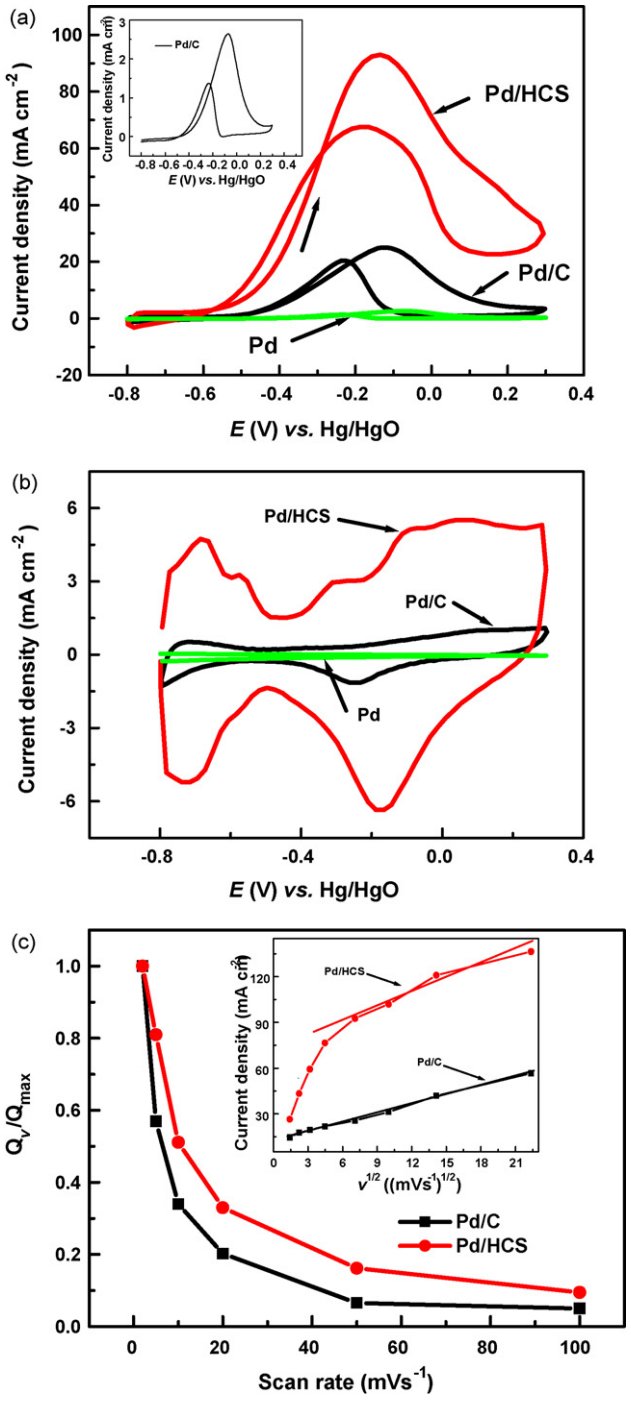

Fig. 5. (a) Cyclic voltammograms of ethanol oxidation on Pd/C and Pd/HCS in 1.0 mol dm^{-3} KOH/1.0 mol dm^{-3} ethanol solution at 303 K, scan rate: 50 mV s^{-1}, (b) cyclic voltammograms of Pd/C and Pd/HCS in 1.0 mol dm^{-3} KOH solution and (c) plot of normalized charge of anodic peak of ethanol oxidation on Pd/C and Pd/HCS electrodes against the scan rate. Inset presents the plots of the peak current density against the square root of the scan rate for both electrodes.

that indicates the characteristic of concentration polarization. However, in the case of Pd/CHS, the data at lower scan rates deviate from the line. The improvement in the mass transport results in a delay of the concentration polarization.

4. Conclusion

Hollow carbon spheres (HCSs) with ultrahigh surface area were prepared by using glucose as carbon source and polystyrene spheres (PSs) as the template. It was found that the addition of poly(ethylene glycol)-block-poly(propylene glycol)-block-poly(ethylene glycol) (P123) during the hydrothermal process could tremendously increase the surface area of the HCS. Ultrahigh surface area of 1249.3 m^2 g^{-1} for the HCS was determined by the BET method which is mainly contributed from the huge micropores. The high surface area of HCS was used as the support of Pd nanoparticles (denoted as Pd/HCS) for ethanol oxidation. It gave more than 5 times higher EASA compared to that of Pd on commercial Vulcan XC-72 carbon at the same Pd loadings. The hollow structure with open micropores and nanochannels leads to the formation of large three-phase interface which is more important for the electrochemical reactions. The high EASA results in a high activity for the ethanol oxidation. This novel electrocatalyst would be a Pt alternative for alcohol oxidation.

Acknowledgments

The authors thank for the financial support given by the NNSF of China (20476108) and the Guangdong Science and Technology Key Project (2007A010700001).

References

[1] D. Ugarte, Nature 359 (1992) 707.
[2] Y. Xiao, Y.L. Liu, L.Q. Cheng, D.S. Yuan, Carbon 44 (8) (2006) 1589.
[3] Y. Xiao, Y.L. Liu, Y.Z. Mi, D.S. Yuan, Chem. Lett. 34 (10) (2005) 1422.
[4] G.F. Zou, J. Lu, D.B. Wang, Inorg. Chem. 43 (2004) 5452.
[5] S. Iijima, Nature 354 (6348) (1991) 56.
[6] S. Frank, P. Doncharal, Z.L. Wang, Science 280 (5370) (1998) 1744.
[7] C. Liu, Y.Y. Fan, M. Liu, H.T. Cong, H.M. Cheng, M.S. Dresselhaus, Science 286 (5442) (1999) 1127.
[8] G.S. Chai, S.B. Yoon, J.H. Kim, J.S. Yu, Chem. Commun. (2004) 2766.
[9] H. Tamai, T. Sumi, H. Yasuda, J. Colloid Interf. Sci. 177 (2) (1996) 325.
[10] F.P. Hu, F. Xiao, J.L. Zhang, X.G. Zhang, Carbon 43 (2005) 2931.
[11] F.P. Hu, F.W. Ding, S.Q. Song, P.K. Shen, J. Power Sources 163 (2006) 415.
[12] Z.Y. Wang, F.P. Hu, P.K. Shen, Electrochem. Commun. 8 (2006) 1764.
[13] F.Y. Xie, Z.Q. Tian, H. Meng, P.K. Shen, J. Power Sources 141 (2005) 211.
[14] Y.Y. Song, Y. Li, X.H. Xia, Electromchem. Commun. 9 (2007) 201.
[15] H.T. Zheng, Y.L. Li, S.X. Chen, P.K. Shen, J. Power Sources 163 (2006) 371.
[16] S.H. Joo, S.J. Choi, I. Oh, J. Kwak, Z. Liu, O. Terasaki, R. Ryoo, Nature 412 (6843) (2001) 169.
[17] H. Meng, P.K. Shen, Electrochem. Commun. 8 (2006) 588.
[18] L. Zhang, J.J. Zhang, D.P. Wilkinson, H.J. Wang, J. Power Sources 156 (2) (2006) 171.
[19] P.K. Shen, C.W. Xu, Electrochem. Commun. 8 (2006) 184.
[20] C.W. Xu, P.K. Shen, Y.L. Liu, J. Power Sources 164 (2007) 527.
[21] O. Savadogo, K. Lee, K. Oishi, S. Mitsushima, N. Kamiya, K.I. Ota, Electrochem. Commun. 6 (2) (2004) 105.
[22] G. Hu, D. Ma, M.J. Chen, L. Li, X.H. Bao, Chem. Commun. 17 (2002) 1948.
[23] L.Q. Xu, W.G. Zhang, Q. Yang, Y.W. Ding, W.C. Yu, Y.T. Qian, Carbon 43 (5) (2005) 1090.

[24] J.W. Liu, M.W. Shao, Q. Tang, X.Y. Chen, Z.P. Liu, Y.T. Qian, Carbon 41 (8) (2003) 1682.
[25] X.G. Yang, C. Li, W. Wang, B.J. Yang, S.Y. Zhang, Y.T. Qian, Chem. Commun. 3 (2004) 342.
[26] Z.Q. Tian, F.Y. Xie, P.K. Shen, J. Mater. Sci. 39 (2004) 1509.
[27] O.D. Velev, P.M. Tessier, A.M. Lenhoff, E.W. Kaler, Nature 401 (6753) (1999) 548.
[28] P.M. Tessier, O.D. Velev, A.T. Kalambur, A.M. Lenhoff, J.F. Rabolt, E.W. Kaler, Adv. Mater. 13 (6) (2001) 396.